KSME

Springer

Journal of Mechanical Science and Technology 37 (2) 2023

Original Article
DOI 10.1007/s12206-023-0112-7

Keywords:
· Finite element analysis
· Hardness
· Mechanically-instrumented indentation test
· Rockwell tester
· Strain hardening modulus

Correspondence to:
Tariq Khraishi
khraishi@unm.edu

Citation:
Li, L., Khraishi, T., Shen, Y.-L. (2023). Investigation of the effect of indentation spacing, edge distance and specimen thickness on the measurement of hardness. Journal of Mechanical Science and Technology 37 (2) (2023) 687~696. http://doi.org/10.1007/s12206-023-0112-7

Received March 8th, 2022
Revised October 16th, 2022
Accepted November 2nd, 2022

† Recommended by Editor Chongdu Cho

Investigation of the effect of indentation spacing, edge distance and specimen thickness on the measurement of hardness

Luo Li, Tariq Khraishi and Yu-Lin Shen

Department of Mechanical Engineering, University of New Mexico, Albuquerque 87131, USA

Abstract Indentation hardness tests are widely used in engineering to test the hardness of a material, which can be performed on a macroscopic scale or microscopic scale. In the present work, copper specimens with different thicknesses were indented with a mechanically-instrumented Rockwell tester. The effects of spacing between indents, indent distance to the edge of the sample, and specimen thickness on the hardness measurement were systematically quantified. Non-linear finite-element modeling was performed, assuming elastic-plastic material response with strain hardening. The two-dimensional numerical modeling of stand-alone and multiple indentations helped to shed more light on the deformation field under indentation, especially the size of the plastic zones and any interaction between them. In addition to the geometric effects, the influence of strain hardening of the test material was also investigated using the finite element analysis. The combined experimental and numerical results provided a range of indent spacings and thicknesses, which yield small to no effect on hardness values. The simulations also quantified the size and shape of the plastic zone under an indent. Lastly, the modeling results showed a competition between the effect of intrinsic material hardening and indent spacing on the value of the measured hardness.

1. Introduction

Indentation related techniques have been extensively used in measuring materials' properties. For instance, hardness tests are used to measure the plastic response of materials [1, 2]. Different types of Indentation tests have been carried out by different researchers for decades. An investigation of hardness and adhesion of sputter-deposited aluminum on silicon by utilizing a continuous indentation test was studied in 1988 [3]. In the following year, fracture toughness of brittle materials by measuring the extent of cracking associated with a Vickers indentations was presented by Ponton et al. [4]. Hutchins et al. in 2018, used an indentation method to determine the interfacial fracture energy for "pop-in" delaminations in a glass-epoxy system [5].

In 2006, Delalleau et al. demonstrated the characterization of the mechanical properties of skin by inverse analysis combined with the indentation test [6]. Over the same period of time, Ogasawara et al. measured the plastic properties of bulk materials by a single indentation test [7]. In the following year, Vickers indentation fracture toughness test was carried out by Quinn et al. [8].

Analysis and simulation of material hardness provide for mechanistic understanding of indentation testing that can work hand-in-hand with experimentation. A new method for the theoretical analysis of static indentation tests was investigated in 1996 [9]. In the same year, analysis of Berkovich indentation using the finite element method was developed by Larsson [10]. Later, a mechanistic analysis of the correlation between overall strength and indentation hardness in discontinuously-reinforced aluminum was shown in 2003 [11]. In 2009, a new optimization algorithm employed for material property evaluation from the indentation test curve was presented [12]. In the following year, numerical analysis for indentation behavior of metal-ceramic

multilayers at nanoscale was carried out by Tang et al. [13]. Another study for the metal-ceramic nanolayered composites using cyclic indentation was reported by Shen et al. [14]. In 2013, hardness estimation for pile-up materials by strain gradient plasticity incorporating the geometrically necessary dislocation density was studied [15]. Hadhri et al. later predicted the hardness of an AISI 4340 steel cylinder using 3D modelling [16]. Some recent simulation studies focused on indentation-induced steady-state metallic creep [17, 18], indentation response affected by undulating multilayers [19], delamination of multilayers [20], shear band formation [21], heterogeneity of living cells [22], and the viscoelastic drift behavior of polymers [23]. The works cited above are only a very small set of an extremely large body of literature about the indentation behavior of materials.

While the indentation hardness testing is straightforward to perform, the measurement result may be influenced by material property, specimen geometry, and test configurations. Care should be taken in interpreting the hardness result. In the present work we attempt to provide a mechanistic basis for the practical hardness information through combined systematic experimental and numerical analyses. The minimum indent spacing, the minimum distance from the indentation center to the specimen edge, and the minimum thickness of the material are assessed by performing extensive mechanically-instrumented indentation tests, for the purpose of quantifying the geometric features which may affect the accuracy of hardness measurement. The common criterion for the indent spacing is that it should be, at minimum, three times the lateral dimension of the indentation to prevent interactions from neighboring indents [24]. However, some researchers also showed that the spacing between two indentation centers can be less than this criterion, or even less than 1.5 indentation diameters [25]. Hence, extensive mechanically-instrumented indentation tests (~200) for different indentation spacings have been undertaken here.

As for the distance from the indentation center to the material edge, the commonly followed criterion for Rockwell hardness test is that it should be a minimum of two and a half indent diameters [24]. To shed light on this criterion, various distances between the indention center and the material edge were employed in the current experimental work.

In addition to the indentation spacing, the authors considered material thickness as another factor that could influence the measured indentation hardness. Hardness tests across 5 different material thicknesses have been carried out to observe how this factor affects the results.

A prior work [25] reported inter-indentation spacing studies using nano-indentations, but attention of the present work is devoted to macro indentations (Rockwell hardness tester). The two studies also use a different indenter tip shape, load and depth for which the physics of scale are not the same. Moreover, the current study considers the variation of the applied load and its consequences. It is the first study, to our knowledge, to employ mechanically-instrumented macro indentation.

In addition, multi-parameter simulations of indentation testing are performed, mimicking the experiments and the ensuing plastic zones, to shed light on the calculated hardness values as affected by plastic zone interactions beneath the indents. This non-linear simulation work was carried out using the ABAQUS finite-element software, taking into account the different hardening moduli to shed light on the effect of material constitutive behavior on indentation hardness results. It is worth mentioning that the effects of indent spacing, material thickness and distance from the material edge have become increasingly important when the material volume to be probed is limited, as in the case of micro devices or miniature components.

2. Experimental details

A main goal of the present work is to demonstrate extensive mechanically-instrumented indentation tests for various indent spacings and different material thicknesses. The Rockwell hardness tester was utilized (Fig. 1). The Rockwell test method is commonly employed for all metals, except for the situations where the test metal structure, or where the indentations, would be too large for the application.

The determination of the Rockwell hardness of a material involves the application of a minor load. The minor load determines the zero position. After the application of the minor load, the major load is applied and then removed, while the minor load remains in place. The depth of penetration from the zero datum is measured from a dial. That is, the indentation depth and hardness are inversely related. The main advantage of Rockwell hardness is its ability to display hardness values directly, thus eliminating tedious calculations involved in other hardness measurement techniques. The equation for Rockwell hardness (HR) calculation is given by [26]:

$$HR = N - hs \tag{1}$$

where h is the indentation depth. N and s are scale factors that

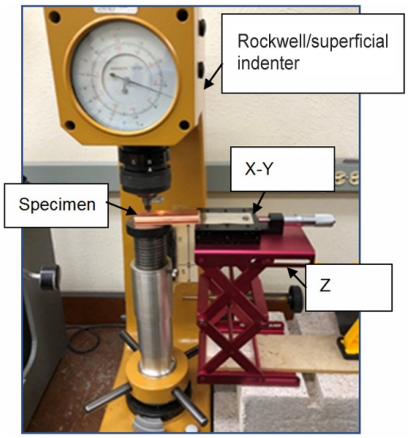

Fig. 1. Experimental setup.

depend on the scale of the Rockwell test being used (for Rockwell F scale: N = 130 and s = 500). By using Eq. (1), one can obtain the indent depth if the hardness is known. Then, the indent diameter can be calculated by using the indent depth and the geometric relationship for a spherical cap shape [27]:

$$r^2 = (r-h)^2 + (0.5d)^2 \tag{2}$$

where r is the radius of the indenter, h is the depth of the indent and d is the indent diameter, since the Rockwell F scale uses a spherical indenter tip.

In addition to the Rockwell indenter, a X-Y stage and Z stage were also employed for this unique experiment as Fig. 1 shows. The Z stage is used to move the X-Y stage in the z-direction. For the X-Y stage, one can use it to move the specimen laterally and longitudinally to ensure accurate indent placement.

In the present indentation study, 110 copper bar material with rounded side edges was chosen (yield strength: 37000 psi = 255.1 MPa). The copper bar was 3 feet long, 1 inch wide and 3/8 inch (9.525 mm) thick. It was cut into several 2-inch-long pieces that remain the same width and thickness as the original copper bar. Some of the specimens were then thinned down into different thicknesses. Also, the rounded side edges were CNC-milled for some of the copper pieces in order to flatten them. In terms of the material properties, the yield strength of 255.1 MPa is based on the property information provided by the vendor (McMaster-Carr [28]). Also, the Rockwell F scale is recommended by the vender for this material.

After the specimens were readied, the study of indent spacing and its effect on hardness was conducted first. In this study, a shim was affixed to the X-Y stage (see Fig. 1). The copper specimen was attached onto the shim with double sided tape, with the shim and the specimen above it sitting on the Rockwell tester anvil (again see Fig. 1). With the X-Y stage, one can ensure the accurate movement of the specimen and perform the indentation test at desired locations. For the indent spacing study, the following center-to-center spacings were used: 3, 2, 1.5 and 1 times the indent diameter.

The same mechanically-instrumented experimental setup (Fig. 1) was used for the studies of the edge effect and the material thickness effect. For the study of the edge effect, the round side edges of the copper specimens were machined off as described above. Additionally, fine grinding was applied to the specimens on their cut side surfaces (which are perpendicular to the top and bottom surfaces experiencing the indents). The necessity for fine grinding will be discussed in Sec. 4. The distance between the indentation center and the material edge is represented by the parameter e. To study the edge effect in the indentation test, one can use the X-Y stage to move the specimen laterally and perform indentations at various e values of 3, 2 and 1 indent diameters from the specimen edge.

For the study of the effect of material thickness on hardness, specimens with different thicknesses were tested in indentation. Here, the copper specimens were thinned down via CNC machining to the following thicknesses: 9.525, 8, 4, 1.880 and 0.940 mm. After thinning, the surfaces to be indented were grinded down using sandpapers (grit #120 and 1000) to remove the effect of any surface hardening due to machining. For this thickness effect, other parameters were held constant. For example, the spacing between indents here was at least 3 times the indent diameter. The distance e during the thickness study was at least 2.5 times the indent diameter. According to Ref. [29], the minimum thickness for the material to ensure thickness-independent results is ten times the indent depth. Therefore, for the first two studies on the effect of indent spacing and the distance to the edge e, the thickness used in the experiments (9.525 mm) met the criterion in this reference.

3. Finite element analysis

Two-dimensional finite element analysis (FEA) was utilized to simulate the indentation test in order to investigate the effect of indent spacing on hardness as well as the plastic zones' interactions beneath the indents. Simulation of the indentations test involves two indents at pre-determined spacing applied one after the other. The software used for this non-linear simulation is ABAQUS.

A finite element mesh with denser elements at the indentation site (see Fig. 2) was applied to the substrate (test material) which has the dimensions of 200 mm (wide)×100 mm (thickness). The element type used was the 4-noded bilinear plane strain element. The number of elements used in the mesh for the simulation was 37500. The copper substrate is elastic-plastic, with Young's modulus of 130 GPa and Poisson's ratio of 0.34 [2].

The plastic response of the copper substrate is dependent on the strain hardening of the material. We employed linear hardening after the initial yield point, and the slope of this linear hardening section is the hardening modulus. Six different hardening moduli were used in the simulation, which are 1 %, 5 %, 10 %, 15 %, 20 % and 25 % of the Young's modulus value.

A semi-spherical indenter geometry was chosen mimicking the spherical Rockwell indenter. The steel indenter is assumed to be linearly elastic, with Young's modulus 215 GPa and Poisson's ratio 0.28 [2].

The indentation test was simulated by moving the semi-spherical indenter into the top face of the substrate. Two load

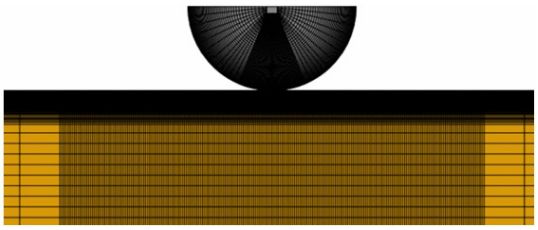

Fig. 2. Finite element model with very fine elements in the upper portion of the substrate near the indentation site.

values were used in the simulations to investigate the effect of loading on the ensuing results, i.e. on the ensuing hardness trends as relating to indent spacing and material properties. One is 600 N and the other is 1200 N. Note that the load-controlled experiment uses 60 kg force for the Rockwell F scale. The bottom boundary of the substrate was fixed in the vertical direction during the indentation. Also, the left bottom corner of the substrate was entirely fixed. The top face of the substrate was not constrained but a friction coefficient of 0.25 was applied for the contact modeling between the indenter and the substrate [30].

In measuring the hardness, the indent diameter (projected contact diameter) in the 2D simulations needs to be determined. Then, one can obtain the projected contact area by multiplying the indent diameter by a unit depth of the substrate following the current 2D simulation setting. Indentation hardness H is calculated via:

$$H = F / A \tag{3}$$

where F is the applied indentation force in the vertical direction and A is the projected contact area. It is important to note that the two-dimensional finite element analysis cannot replicate the conditions of a real three-dimensional indentation test. Nonetheless, the objective of this simulation is to facilitate a direct but qualitative comparison to the experimental results.

4. Results and discussion

4.1 Experimental results

4.1.1 Indent spacing

Fig. 3 shows the images from indentation tests at different indent spacings.

These pictures are zoomed in and are all away from the specimen edges.

The Rockwell F hardness results for the indentations in Figs. 3(a)-(d), are plotted in Fig. 4 for the mean values and associated error bars exhibiting the experimental scatter. As Fig. 4 shows, the hardness increases with decreasing indent spacing. This is hypothesized as the plastic zones under them tend to overlap and thus produce harder response. This physical phenomenon can be revealed clearly using simulations presented later in this paper. The figure also shows that the hardness values tend to stabilize around 3 indent diameters spacing. However, taking into account the scatter in the data, there is not a significant change in the hardness values from the lowest to the highest average results (a difference of about 2 % maximum).

To further explore the plastic zone interaction effect on the hardness values, the authors did a row of indentations that were 1 indent (center-to-center) apart. This is the bottom row in Fig. 3(e). Then another row of indents was carried out (the top row in Fig. 3(e)). Lastly, the middle row of indents in the figure was made and the hardness calculated. This allowed for up to five interactions between indent plastic zones versus the one interaction present in one row of indents. On average for this middle row, the measured hardness was 87.06 HRF which was higher than the 84.04 HRF for the one isolated row of indents (Fig. 3(d)) with 1 indent diameter spacing. Comparing the last two numbers, there is a difference now of about 6 % indicating that more indents surrounding a new indent will cause the hardness value to go up. In other words, there are more plastic zones interacting with each other beneath the indentations in Fig. 3(e) than in Fig. 3(d).

(a) Indentation test at 3 indent diameters spacing for 9.525-mm-thick copper (1 row)

(b) Indentation test at 2 indent diameters spacing for 9.525-mm-thick copper (1 row)

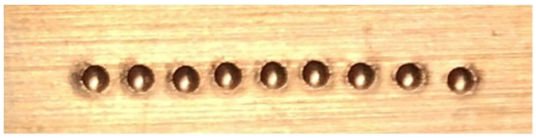

(c) Indentation test at 1.5 indent diameters spacing for 9.525-mm-thick copper (1 row)

(d) Indentation test at 1 indent diameter spacing for 9.525-mm-thick copper (1 row)

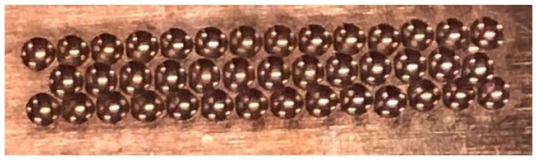

(e) Indentation test at 1 indent diameter spacing for 9.525-mm-thick copper (3 rows)

Fig. 3. Indentation images.

4.1.2 Specimen thickness

As the material thickness decreases, it is expected that the hardness values would differ significantly from bulk values. This could be due to either less resistance encountered inside the material towards the indentation force since less material can experience plastic hardening or because more resistance might be felt from the hard tester base, i.e., anvil, upon which the specimen lies. Such possibilities can lead to inaccurate test results. According to Fig. 5, the hardness slightly goes up, then

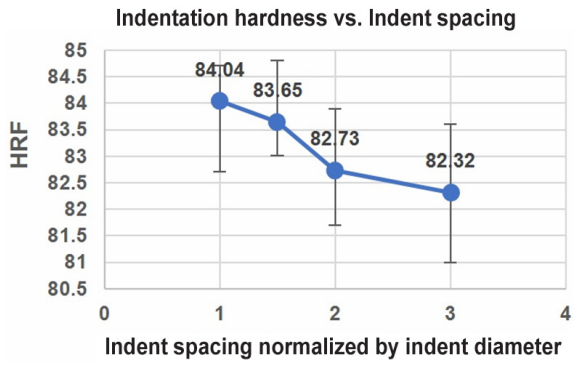

Fig. 4. Indentation test results at different indent spacings for 9.525-mm-thick copper (mean value is averaged over 40 points or hardness tests for each indent spacing).

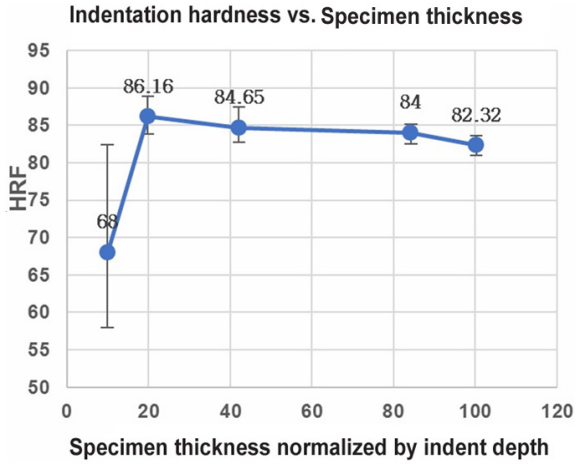

Fig. 5. Indentation test results for different copper specimen thicknesses.

down as the material thickness decreases. The figure shows that when the thickness decreases, the effect of the anvil is felt more and more but at very small thicknesses there is not much material left to resist the indentation (i.e., to cause an increase in hardness). The figure shows that anything above a normalized thickness value of 40 should be sufficient for this type of indentation testing, i.e., the hardness values stabilize after this thickness. It is important to mention again here that the indent depth is calculated from Eq. (1) using the hardness value.

4.1.3 Distance from the indentation center to the material edge

If one indents close to the specimen edge, hardness values are expected to decline due to less material resistance since less plastic zone can form there. However, this experiment employed a rounded edge copper bar. Hence, the rounded edges were CNC-milled as mentioned above. The work hardening caused by machining will influence the hardness results as a function of *e*. To remove the effect of work hardening, we performed fine grinding on the cut surfaces before the hardness testing. This yielded the expected behavior as Fig. 6 shows. The figure shows that, once the *e* value is 2 or higher,

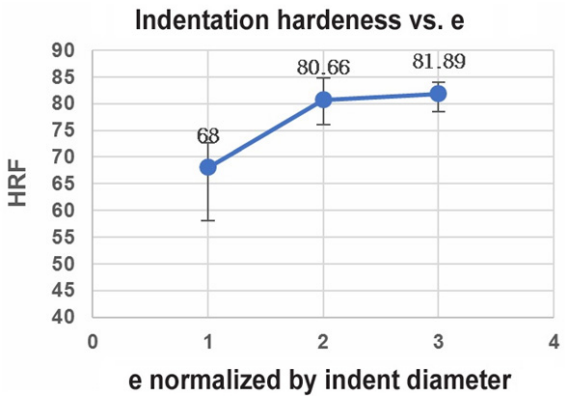

Fig. 6. Indentation test results at different *e* values for 9.525-mm-thick copper.

Fig. 7. This figure shows *e* equal to 2 indentation diameters for the 9.525-mm-thick copper.

the hardness values tend to stabilize. Fig. 7 shows indents close to the flat side edge of the specimen for one exemplary *e* value.

4.2 Simulation results

4.2.1 Effect of indent spacing on hardness

The simulations all started with one indentation, while calculating its corresponding hardness value, followed by a second indentation. The second indentation was spaced 1 indent diameter, 2 indent diameters or 3 indent diameters from the first indent. Fig. 8 shows an example of one indent (Fig. 8(a)) followed by a second indent (Fig. 8(b)) with the 2 indent diameter spacing. The color contours represent the equivalent plastic strain. This figure is exemplary of what is seen in the different cases: the plastic zone of the second indent interacts with the plastic zone of the first indent affecting the calculated hardness in the process.

Fig. 9 shows the calculated second indentation hardness as a function of the indent spacing. The hardness is seen to increase as the indent spacing decreases, which is consistent with the experimental indentation test results. Next, the second indentation hardness was normalized by the first indentation (i.e., the non-interacting indentation) hardness in order to study the deviation of the indentation hardness as one varies the indent spacing. As Fig. 10 shows, the indentation hardness for the 1-indent-diameter spacing is the highest followed by the 2-indent-diameter spacing and then the 3-indent-diameter spacing. The 3-indent-diameter spacing is equal to the stand-alone indentation; the modeling thus suggests that, at this spacing or more, the hardness measurement is not affected by nearby

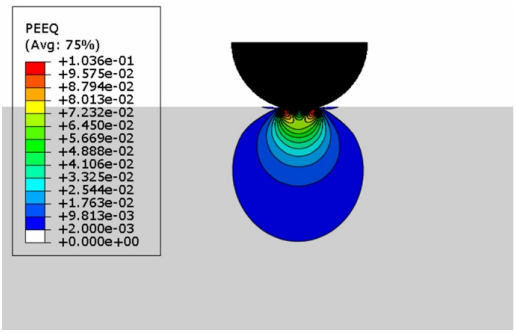

(a)

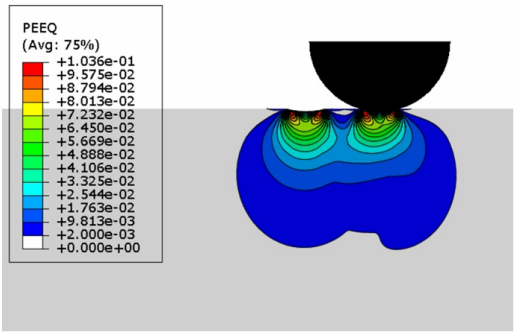

(b)

Fig. 8. Equivalent plastic strain contours for 600 N constant load, using 5 % hardening modulus for the strain hardening response of the material: (a) first indent; (b) second indent (at 2-indent-diameter spacing).

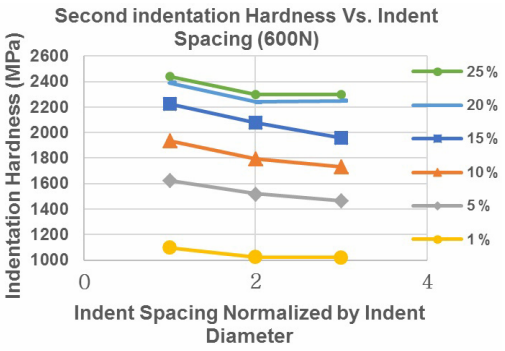

Fig. 9. Simulation results (second indentation hardness vs. normalized indent spacing) for various hardening moduli and 600 N constant load.

indents.

As the hardening modulus increases from 1 % upwards, the normalized indentation hardness increases as well. This is expected since in the limit of 0 % hardening modulus, no interaction of the plastic zones is expected (due to no physical hardening happening between dislocation-induced plasticity [31]). That interaction should increase with increased internal hardening in the material. The hardening modulus of 15 % exhibits the highest increase in normalized hardness values as the indent spacing is decreased (Fig. 10). After the 15 % hardening modulus, however, the normalized hardness values decrease. This is also expected, as in the limit of 100 % hardening modulus, the material becomes essentially elastic so there

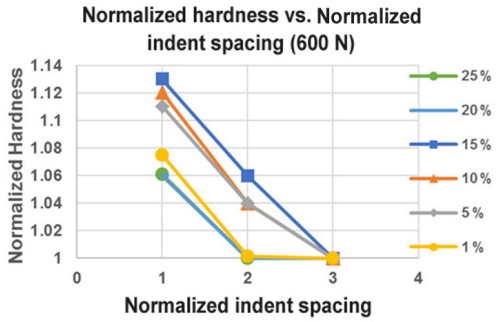

Fig. 10. Normalized hardness (second indentation hardness is normalized by the first indentation hardness) vs. normalized spacing (normalized by indent diameter) for 6 different hardening moduli (percent of Young's modulus) and 600 N constant load (Note that the results of 20 % and 25 % are on top of each other).

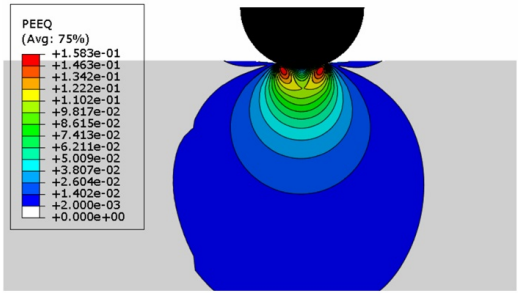

(a)

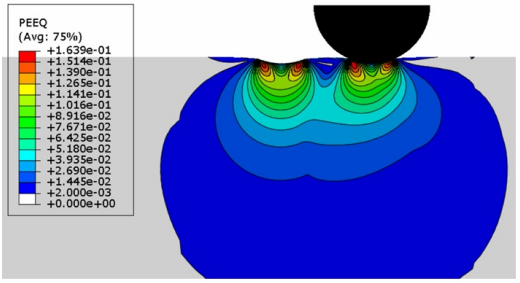

(b)

Fig. 11. Equivalent plastic strain contours for 1200 N constant load and 5 % hardening modulus: (a) first indent; (b) second indent (at 2-indent-diameter spacing).

is essentially no plastic zones to interact. Sec. 4.2.3 further elaborates on this plastic zone size effect.

The same simulation process was repeated with a different constant load (1200 N) in order to capture the effect of the indentation load. Fig. 11 shows an example of the contour plots under indentation. We contrast the plastic zone sizes in Figs. 8 and 11. Fig. 11 shows that the indent size (diameter in real testing) and the associated plastic zone both increase in value as the indent load is increased. Fig. 11(b) for 1200 N is similar to Fig. 8(b) for 600 N in the sense that they both show the interacting plastic zones beneath the indented surface due to other nearby indents.

Figs. 12 and 13 are similar to Figs. 9 and 10 but with results for the 1200 N load instead of 600 N. The hardness values in

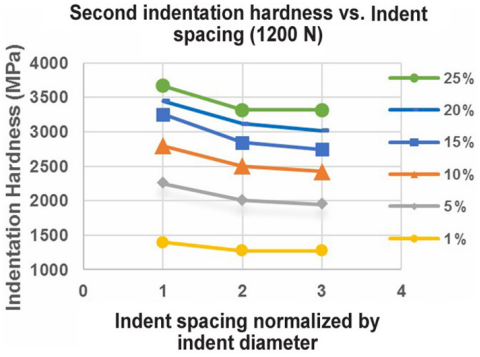

Fig. 12. Simulation results (second indentation hardness vs. normalized indent spacing) for various hardening moduli and 1200 N constant load.

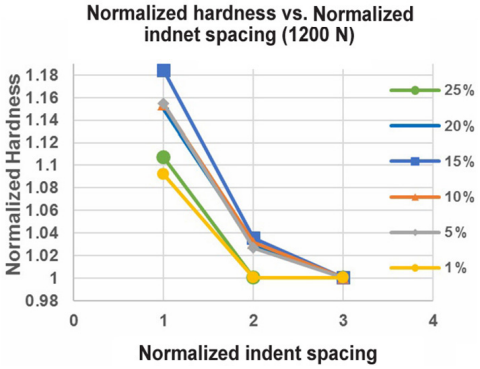

Fig. 13. Normalized hardness (second indentation hardness is normalized by the first indentation hardness) vs. normalized spacing (normalized by indent diameter) for 6 different hardening moduli and 1200 N constant load.

MPa for 1200 N are larger than for 600 N. The normalized hardness in Fig. 13 is higher than that in Fig. 10, indicating that the plastic zone interactions with the higher indentation load are stronger and hence the normalized hardness is higher than for 600 N. Another important observation from Fig. 13 is that, similar to Fig. 10, a 3-indent-diameter spacing is sufficient to produce hardness results that are not affected by other nearby indents.

4.2.2 Plastic zones interactions

In this sub-section, the authors present contour plots for a chosen hardening modulus (25 %) in order to show how, for the same applied indentation load, more interaction between the indentation plastic zones result in higher hardness values for the second indent. Note that, for the same 1200 N load, the indentation depth and diameter for 25 % hardening modulus (Fig. 14(b)) are smaller than for 5 % hardening modulus (Fig. 11(b)). This leads to, for the 2-indent-diameter spacing, a 0 % hardness deviation between the second indent over the first indent for 25 % hardening modulus, as opposed to a 2.67 % hardness deviation between the second indent over the first indent for 5 % hardening modulus (see Fig. 13).

4.2.3 Plastic zone size

For a single indentation, the plastic zone under the indenter

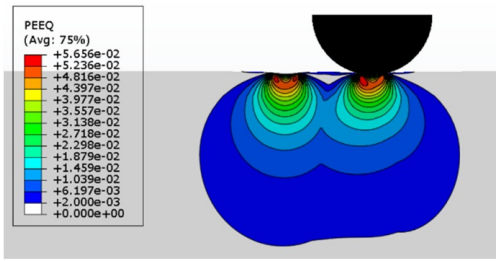

(a) Hardness deviation: 0 % (3 indent-diameter-spacing)

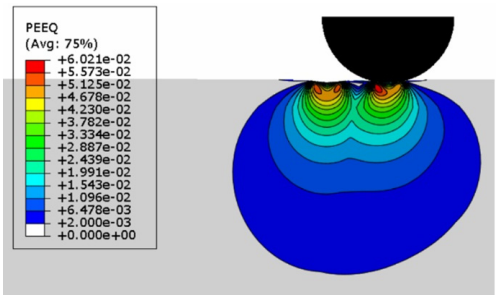

(b) Hardness deviation: 0 % (2 indent-diameter-spacing)

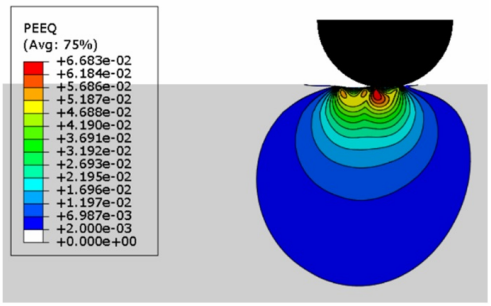

(c) Hardness deviation: 10.7 % (1 indent-diameter-spacing)

Fig. 14. The plastic zones beneath the indents at various indent spacings for a hardening modulus of 25 % and 1200 N indentation load.

exhibits a more or less circular shape. To quantify this shape, two dimensions are measured: the width of the zone D1 and the distance from the indented surface to the bottom of the zone D2 (see Fig. 15, and Tables 1 and 2). The units of D1 and D2 are both 10^{-4} m. The table shows the diameters in measured units and also as normalized values D1* and D2* (D1 normalized with respect to the indent diameter, and D2 with respect to the indent depth, respectively). H' is the hardening modulus. According to Table 1, the plastic zone induced by the indent is roughly a circle. The zone is smaller for a material with a higher hardening modulus, which implies that there is less zone interaction for the hard material (See the discussion in Subsec. 4.2.1). However, for materials with higher hardening moduli, as the figures before (Figs. 12 and 9) showed, the material expectedly measures higher hardness values.

As a consequence, there is a competition between diminishing plastic zone size and interaction with higher hardening moduli resulting in smaller normalized hardness values for the second indent, and between increasing hardness values due to higher hardening moduli. This competition is responsible for

Table 1. Plastic zone dimensions for various hardening moduli (for 600 N).

H'	5 %	10 %	15 %	20 %	25 %
D1 (units)	152.6	133.2	123.5	113.9	108.1
D2 (units)	156.4	137.3	127.7	118.0	108.2
D1*	3.7	3.8	4	4.3	4
D2*	37.2	41.6	44	45.3	45.4

Table 2. Plastic zone dimensions for various hardening moduli (for 1200 N).

H'	5 %	10 %	15 %	20 %	25 %
D1 (units)	322.6	280	253.0	235.5	222
D2 (units)	340	293	264.2	245	230
D1*	5.3	5.6	5.8	5.9	6.1
D2*	32.4	37.6	40.0	41.5	42.6

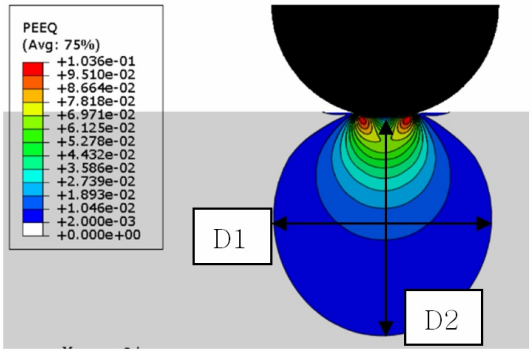

Fig. 15. Plastic zone size beneath the indent.

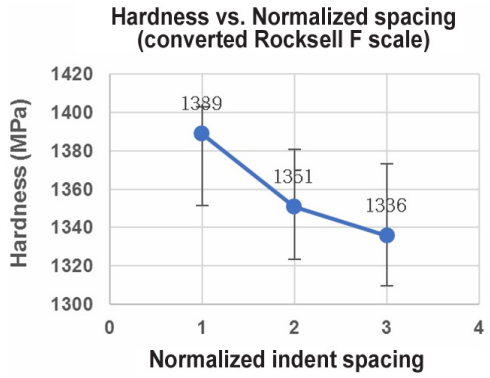

(a) Indentation test results (in MPa) at different indent spacings for 0.375-inch-thick copper

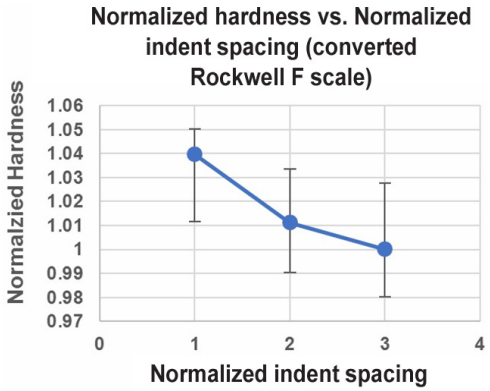

(b) Normalized hardness from Fig. 16(a) at different normalized indent spacings. The hardness was normalized by the hardness value at 3-indent-diameters spacing

Fig. 16. Indentation test results converted into MPa and then normalized.

first an increase in the value of normalized hardness with the hardening modulus, up to 15 % hardening moduli, and then a decrease (see Figs. 10 and 13).

Tables 1 and 2 also reveal that, using a plastic strain threshold of 0.2 %, the lateral size of the plastic zone is about 4 times the indent diameter and up to about 6 times. This indicates that when indenting, and to ensure no interaction of the plastic zone with sides of the specimens (free surfaces or surfaces in contact with other things), one needs to account for this lateral dimension below the indent surface in order to achieve hardness values that are not skewed in values. This can be gleaned from Fig. 6 for the experiments. A similar observation can be made about the depth dimension from the D2* values. The depth of the indented specimen needs to be at least about 40 times the indent depth for accurate hardness readings. This is in agreement with the experimental hardness measurement in Fig. 5.

4.2.4 Comparing experimental and modeling hardness values

The hardness results obtained from the indentation test were in the Rockwell F scale (HRF), which were converted into units of MPa to compare with the simulation results. To perform the conversion from HRF to MPa, one can calculate the indent depth from Eq. (1) based on HRF. Then, the indent diameter can also be obtained from Eq. (2). Once the indent diameter is known, the indent area can be obtained immediately since the indenter is spherical. The hardness in units of MPa can then be developed using Eq. (3). The experimental data in Fig. 16(a) is within the data range for the simulations in Fig. 9 and also showing a similar upward trend with decreasing distance between indents. Moreover, the normalized hardness results in Fig. 16(b) also shows a similar trend to Fig. 10 but more on the low-end for the 1-indent-diameter spacing. Overall, it is to be cautioned that comparing 2D simulation results to 3D experimental hardness results is not expected to generate quantitative agreement. The comparison is more qualitative in nature but it can shed some light on the plastic zone size, shape and interactions. This qualitative agreement lends credibility to the general approach used in this work.

5. Conclusions

The mechanically-instrumented Rockwell indentation tests for 110 copper were undertaken, along with 2D non-linear finite-element simulations of elastic-plastic material with various

linear hardening moduli under different indentation loads. Salient findings are summarized below.

1) Hardness increases with decreasing indentation spacing, due to the plastic zones under the nearby indents overlapping and thus producing a harder response.

2) No significant changes in hardness values occur unless the indent spacing is less than 2-indent-diameters.

3) For hardness values independent of the plastic zone interaction or specimen edge effect, it is better to aim at an indent spacing equal to four diameters.

4) The size of the plastic zone decreases with increased strain hardening, with the zone shape very close to a circle.

5) The thickness of the indented specimen, as shown by the modeling and the experiments, should be on the order of 40 indent depths to minimize any effect from the supporting platform underneath the specimen.

6) The numerical modeling results demonstrated that there is a certain material hardening modulus (equal to 15 % of the Young's modulus) which corresponds to the highest increase in normalized hardness with decreased indent spacing. This increasing trend diminished if the hardening modulus is above or below the 15 % case.

Acknowledgments

The authors would like to thank the University of New Mexico's (UNM) Mechanical Engineering Department for supporting this research work.

References

[1] D. Tabor, *The Hardness of Metals*, Clarendon Press, Oxford (1951).

[2] W. D. Callister and D. G. Rethwisch, *Materials Science and Engineering: An Introduction*, 8th Ed., Wiley, New York (2009).

[3] D. Stone, W. LaFontaine, P. Alexopoulos, T. Wu and C. Li, An investigation of hardness and adhesion of sputter-deposited aluminum on silicon by utilizing a continuous indentation test, *Journal of Materials Research,* 3 (1) (1988) 141-147.

[4] C. B. Ponton and R. D. Rawlings, Vickers indentation fracture toughness test part 1 review of literature and formulation of standardised indentation toughness equations, *Materials Science and Technology*, 5 (9) (1989) 865-872.

[5] K. Hutchins, T. Buchheit, R. Tandon and T. Khraishi, Determination of interfacial fracture energy for pop-in delaminations in a glass-epoxy system using the indentation method, *Journal of Theoretical and Applied Multiscale Mechanics*, 3 (2) (2018) 116-126.

[6] A. Delalleau, G. Josse, J. M. Lagarde, H. Zahouani and J. M. Bergheau, Characterization of the mechanical properties of skin by inverse analysis combined with the indentation test, *Journal of Biomechanics*, 39 (9) (2006) 1603-1610.

[7] N. Ogasawara, N. Chiba and X. Chen, Measuring the plastic properties of bulk materials by single indentation test, *Scripta Materialia*, 54 (1) (2006) 65-70.

[8] G. D. Quinn and R. C. Bradit, On the Vickers indentation fracture toughness test, *Journal of the American Ceramic Society*, 90 (3) (2007) 673-680.

[9] M. Sakamoto, G. Li, T. Hara and E. Y. S. Chao, A new method for theoretical analysis of static indentation test, *Journal of Biomechanics*, 29 (5) (1996) 679-685.

[10] P. L. Larsson, A. E. Giannakopoulos, E. Söderlund, D. J. Rowcliffe and R. Vestergaard, Analysis of Berkovich indentation, *International Journal of Solids and Structures*, 33 (2) (1996) 221-248.

[11] B. D. Kozola and Y.-L. Shen, A mechanistic analysis of the correlation between overall strength and indentation hardness in discontinuously reinforced aluminum, *Journal of Materials Science,* 38 (2003) 901-907.

[12] A. Biabangard-Oskouyi, E. Atashpaz-Gargari, N. Soltani and C. Lucas, Application of imperialist competitive algorithm for materials property characterization from sharp indentation test, *International Journal of Engineering Simulation*, 10 (1) (2009) 11-12.

[13] G. Tang, Y.-L. Shen, D. R. P. Singh and N. Chawla, Indentation behavior of metal-ceramic multilayers at the nanoscale: numerical analysis and experimental verification, *Acta Materialia,* 58 (6) (2010) 2033-2044.

[14] Y.-L. Shen, C. B. Blada, J. J. Williams and N. Chawla, Cyclic indentation behavior of metal-ceramic nanolayered composites, *Material Science and Engineering A,* 557 (2012) 119-125.

[15] M. S. Park and Y. S. Suh, Hardness estimation for pile-up materials by strain gradient plasticity incorporating the geometrically necessary dislocation density, *J. Mech. Sci. Technol.,* 27 (2013) 525-531.

[16] M. Hadhri, A. El Ouafi and N. Barka, Prediction of the hardness profile of an AISI 4340 steel cylinder heat-treated by laser - 3D and artificial neural networks modelling and experimental validation, *J. Mech. Sci. Technol.,* 31 (2017) 615-623.

[17] M. E. Cordova and Y.-L. Shen, Indentation vs. uniaxial power-law creep: a numerical assessment, *Journal of Materials Science*, 50 (2015) 1394-1400.

[18] N. J. Martinez and Y.-L. Shen, Analysis of indentation-derived power-law creep response, *Journal of Materials Engineering and Performance*, 25 (2016) 1109-1116.

[19] R. D. Jamison and Y.-L. Shen, Indentation and overall compression behavior of multilayered thin-film composites: effect of undulating layer geometry, *Journal of Composite Materials*, 50 (4) (2016) 507-521.

[20] R. D. Jamison and Y.-L. Shen, Delamination analysis of metal-ceramic multilayer coatings subject to nanoindentation, *Surface and Coatings Technology*, 303A (2016) 3-11.

[21] S. Bigelow and Y.-L. Shen, Parametric computational analysis of indentation-induced shear band formation in metal-ceramic multilayer coatings, *Surface and Coatings Technology*, 350 (2018) 779-787.

[22] G. Tang, M. Galluzzi, B. Zhang, Y.-L. Shen and F. Stadler, Biomechanical heterogeneity of living cells: comparison between atomic force microscopy and finite element simulation, *Langmuir*, 35 (2019) 7578-7587.

[23] Y.-L. Shen, On the viscoelastic drift behavior during nanoindentation, *Frontiers in Materials*, 9 (2022) 900088.
[24] EMCO-TEST, *General Tips. Minimum Distance between Test Points and to the Specimen Edge*, EMCO-TEST Prüfmaschinen GmbH, https://www.emcotest.com/en/the-world-of-hardness-testing/hardness-know-how/applications-tips/general-tips/minimum-distance-between-test-points-and-to-the-specimen-edge/.
[25] P. S. Phani and W. C. Oliver, A critical assessment of the effect of the indentation spacing on the measurement of hardness and modulus using instrumented indention testing, *Journal of Materials and Design*, 164 (2009) 107563.
[26] T. Khraishi and M. S. Al-Haik, *Experiments in Materials Science and Engineering*, Cognella, Solana Beach (2011).
[27] J. W. Harris and H. Stocker, *Handbook of Mathematics and Computational Science*, Springer, New York (1998).
[28] McMaster-Carr, *Multipurpose 110 Copper Bars with Rounded Edges*, McMaster-Carr Supply Company (2022) https://www.mcmaster.com/copper/multipurpose-110-copper-bars-with-rounded-edges-9/.
[29] EMCO-TEST, *Rockwell Method, Minimum Specimen Thickness*, EMCO-TEST Prüfmaschinen GmbH (2022) https://www.emcotest.com/en/the-world-of-hardness-testing/hardness-know-how/applications-tips/general-tips/rockwell-method-minimum-specimen-thickness/.
[30] J. L. Bucaille, S. Stauss, E. Felder and J. Michler, Determination of plastic properties of metals by insutrmented indentation using different sharp indenters, *Journal of Acta Materialia,* 51 (6) (2003) 1663-1678.
[31] A. B. Siddique, H. Lim and T. A. Khraishi, The effect of multipoles on the elasto-plastic properties of a crystal: theory and three-dimensional dislocation dynamics modeling, *Journal of Engineering Materials and Technology*, 144 (1) (2022) 011016.

Luo Li is a Ph.D. student in the Mechanical Engineering Department at the University of New Mexico. His research interests include materials science with emphasis on mechanical properties and characterization, mechanics of materials, composite materials, and advanced manufacturing.

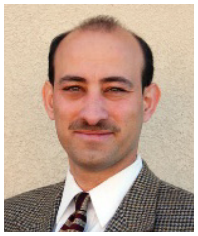

Tariq Khraishi is currently a Professor of Mechanical Engineering at the University of New Mexico, U.S.A. He received his Ph.D. in Engineering from Washington State University. His research work is in the general areas of mechanics and materials science. In particular he has performed modelling, theoretical and/or experimental research in biomechanics, dislocation dynamics, eigenstrain theory/modelling, fracture mechanics, nano structures, irradiation damage, void growth/interaction in superplasticity, and stresses in thin films.

Yu-Lin Shen is currently a Professor and Chair of the Department of Mechanical Engineering at University of New Mexico, U.S.A. He received his Ph.D. in Engineering from Brown University. His research areas include mechanical behavior of materials and solid mechanics, with particular interests in applying modeling techniques to address micro-mechanical problems related to thin films, microelectronic devices and packages, and composite materials.